frontiers | Frontiers in Earth Science

TYPE Original Research
PUBLISHED 30 January 2023
DOI 10.3389/feart.2023.1112067

OPEN ACCESS

EDITED BY
Haopeng Geng,
Lanzhou University, China

REVIEWED BY
Kai Cao,
China University of Geosciences Wuhan, China
Fenliang Liu,
Hunan City University, China

*CORRESPONDENCE
Dario Gioia,
dario.gioia@cnr.it

SPECIALTY SECTION
This article was submitted to Quaternary Science, Geomorphology and Paleoenvironment, a section of the journal Frontiers in Earth Science

RECEIVED 30 November 2022
ACCEPTED 19 January 2023
PUBLISHED 30 January 2023

CITATION
Gioia D, Corrado G, Danese M, Minervino Amodio A and Schiattarella M (2023), Post-lacustrine evolution of a tectonically-controlled intermontane basin: Drainage network analysis of the Mercure basin, southern Italy. *Front. Earth Sci.* 11:1112067. doi: 10.3389/feart.2023.1112067

Post-lacustrine evolution of a tectonically-controlled intermontane basin: Drainage network analysis of the Mercure basin, southern Italy

Dario Gioia[1]*, Giuseppe Corrado[2], Maria Danese[1], Antonio Minervino Amodio[1] and Marcello Schiattarella[2]

[1]Consiglio Nazionale delle Ricerche—Istituto di Scienze del Patrimonio Culturale (ISPC), Tito Scalo, Potenza, Italy, [2]Università della Basilicata, Dipartimento delle Culture Europee e del Mediterraneo (DiCEM), Matera, Italy

Topographic analysis, drainage network morphometry, river profile analysis, and spatial distribution of fluvio-lacustrine terraces have been used to reconstruct the drainage network evolution in the Mercure River basin, a large intermontane tectonic basin of the axial zone of southern Apennines. Morphotectonic evolution of the study area is mainly controlled by poly-kinematics high-angle WNW-ESE and NE-SW faults, which promoted the development of a complex landscape with relict landscapes and/or low-relief erosional surfaces that occurred in a staircase arrangement at the top of the landscapes or at higher altitudes than the basin infill. The creation of the accommodation space for the deposition of the thick basin infill was related to an important tectonic phase of block-faulting along N120°-trending normal faults, which occurred in the final part of the Lower Pleistocene. Such an evolution strongly controls the longitudinal profile forms of channels draining the northern sector of the study area, which are featured by a well-developed concave-up segment in river profiles of these channels between an upward trait with lower values of channel steepness and the trace of the master fault. River profiles in north-western and south-east sectors of the Mercure River basin exhibit clear knickpoints at altitudes comparable with those of the superimposed orders of relict landscapes related to the initial formation of the tectonic basin and the subsequent evolution of the endorheic basin, with a post-lacustrine geomorphological evolution of the drainage network that is controlled by fluvial incision occurring at rates comparable than those reconstructed by independent morphotectonic markers. The erosion of the threshold of the endorheic basin occurring during the base-level fall of the MIS 12 promoted a dramatic base-level fall of about 150 m, which corresponds to a mean incision rate of about 0.35 mm/yr. Post-lacustrine evolution of the Mercure basin strongly controls the morphometric features of the drainage network, which preserves a centripetal pattern with several planimetric anomalies such as counterflow and high-angle confluences, local-scale fluvial capture phenomena and drainage divide migrations.

KEYWORDS

tectonic geomorphology, river profile analysis, fault-bounded intermontane basin, base-level changes, southern Italy, drainage network changes

1 Introduction

Lake overflow or, in general, a transition from endorheic to exorheic condition have a dramatic impact on a landscape due to the sudden base-level fall that promoted a fast re-organization of the drainage network and deep fluvial incision (Ben Moshe et al., 2008; Vacherat et al., 2018; Poeppl et al., 2019; Gioia and Schiattarella, 2020). Although the analysis of the long-term response of a transient landscape to the change from lacustrine conditions to drainage integration can be crucial to understand the evolution of fluvial systems with a high degree of disequilibrium, few studies have investigated the complex relationships between base-level lowering induced by post-lacustrine evolution of a landscape and the geomorphic response of the drainage network. In addition, such works are mainly focused on the identification of the mechanism of drainage integration (Hilgendorf et al., 2020) or on intracontinental endorheic basins (Cunha et al., 2019; Soria-Jáuregui et al., 2019; Struth et al., 2019). In the last years, there is a growing interest on such a topic (see for example Dorn et al., 2020; Gioia and Schiattarella, 2020; Larson et al., 2020; Skotnicki et al., 2021; Gootee et al., 2022; Larson et al., 2022). Recent works highlighted that an endorheic/exorheic transition promoted a complex and fast topographic, erosional, and depositional re-organization of a landscape (Larson et al., 2022) but several open problems such as the impact of climate changes on drainage integration processes need to be better investigated (Hilgendorf et al., 2020; Larson et al., 2022). In addition, few comprehensive studies deal with the estimation of long-term rates of fluvial incision and knickpoint migration induced by a sudden base-level lowering. River profile analysis can represent one of the most powerful tools to reconstruct the landscape response to perturbations induced by tectonic and climate forces (Pritchard et al., 2009; Kent et al., 2017; Struth et al., 2019; Armstrong et al., 2021; Marra et al., 2022) and similar investigation on modalities and rates of knickpoint migration in response to drainage integration can be useful to improve our knowledge about the mechanisms of re-arrangement of a fluvial system during a fast endorheic/exorheic transition. The axial zone of the southern Apennines (Figure 1) can potentially represent a key sector for the investigation of drainage network evolution in response to endorheic-exorheic transition since it is featured by several Quaternary intermontane basins with a well-constrained morpho-stratigraphic record of transition from lacustrine to fluvial deposition (Aucelli et al., 2014; Schiattarella et al., 2017). Quaternary tectonics created the accommodation space for the generation of several larger intermontane basins in the axial zone of the orogen, such as the Auletta, Vallo di Diano, Agri, Noce and Mercure basins (Schiattarella et al., 1994; Zembo, 2010; Gioia et al., 2011; Schiattarella et al., 2013; Giano et al., 2014; Schiattarella et al., 2017). Among them, the Mercure basin represents a relevant case study where one can investigate the long-term response of the drainage network to a transition from endorheic to exorheic conditions. In fact, the study area (Figure 2) is a tectonically-controlled basin with a well-constrained morphotectonic and morpho-stratigraphic evolution (Schiattarella et al., 1994; Marra, 1998; Giaccio et al., 2014; Robustelli et al., 2014). Apart from a well-reconstructed chronological history of lacustrine deposition, the study area is a good example of a transient landscape showing clear geomorphological evidences of relict stages of geomorphological evolution such as superimposed orders of erosional surfaces and fluvio-lacustrine terraces, drainage network anomalies and river profile knickpoints/knickzones. We use topographic analysis, drainage network morphometry, river profile analysis, spatial distribution of fluvial terraces, and lacustrine depositional tops to infer the post-lacustrine geomorphological evolution of the drainage network. Integration between such data and classical morphotectonic analysis allowed us to reconstruct: i) The palaeodrainage of the endorheic stage of the basin and the drainage network evolution after the onset of the exorheic condition; ii) the post-lacustrine evolution of the drainage network and rates of incision and knickpoint retreat.

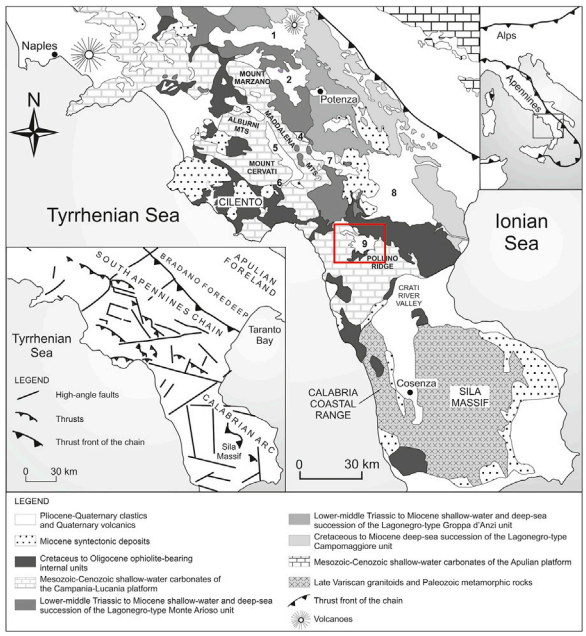

FIGURE 1
Geological sketch map of the Campania-Lucania Apennine and Northern Calabria. In the frame, main tectonic structures are reported. Toponyms of the intermontane basins (indicated with numbers): 1: Ofanto basin; 2: Tito-Picerno basin; 3: Auletta basin 4: Pergola-Melandro basin; 5: Vallo di Diano basin; 6: Sanza basin; 7: Agri basin; 8: Sant'Arcangelo basin; 9: Mercure basin. Modified after Schiattarella et al. (2017).

2 Regional and local setting

The southern Apennines (Figure 1) are a northeast-verging fold-and-thrust belt (Menardi Noguera and Rea, 2000) with a Quaternary evolution strongly controlled by regional uplift and block-faulting (Schiattarella et al., 2003). As a result, the Oligocene-Pliocene contractional structure was dismembered by impressive WNW-ESE and NE-SW high-angle fault systems, which showed a complex kinematic history and created the accommodation space for the creation of several larger intermontane basins. The morpho-sedimentary evolution of some of these basins (i.e., Mercure, Noce, Agri and Vallo di Diano basins) is featured by endorheic conditions during Lower-Middle Pleistocene, mainly related to an increase in fault activity (Schiattarella et al., 2017). The mountain belt tops of the axial zone are frequently characterized by a low-relief topography representing remnants of an ancient (i.e., late Pliocene in age, (Schiattarella et al., 2013; Schiattarella et al., 2017), planation landscape. Fault activity promoted the displacement of the summit

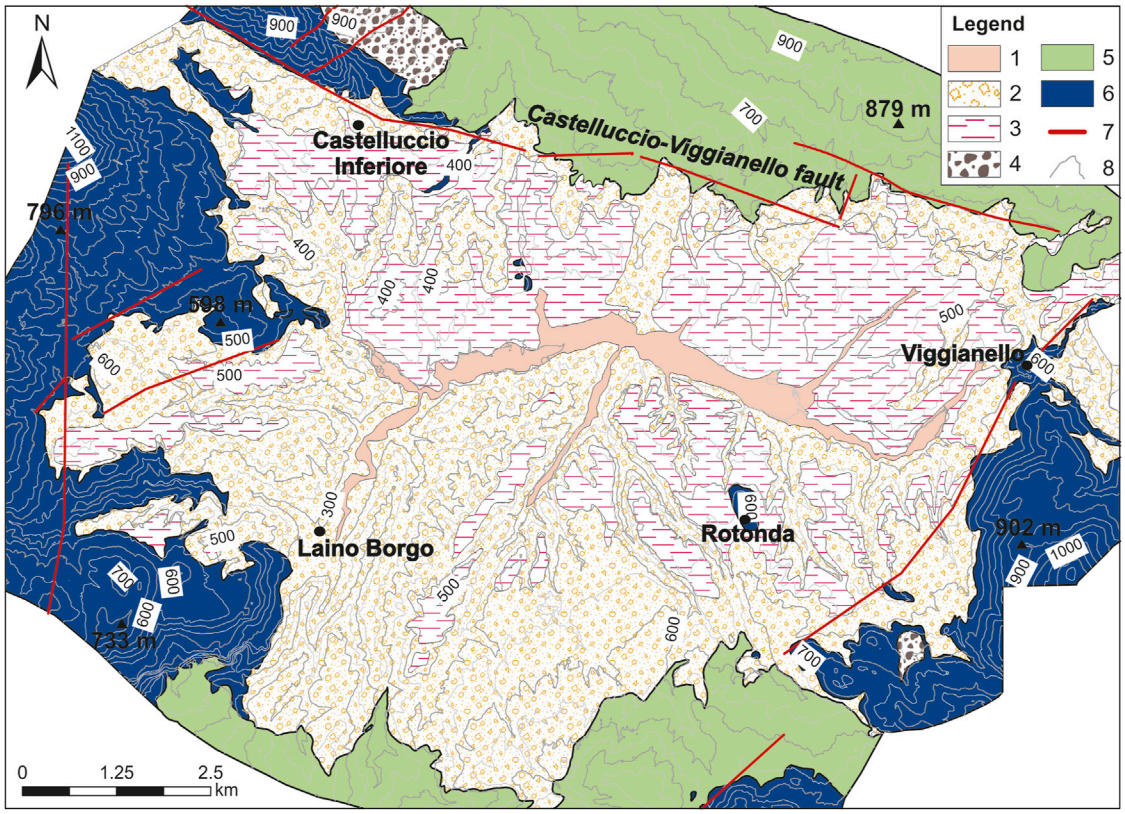

FIGURE 2
Geological map of the Mercure River basin. 1) Present-day alluvial deposits; 2) Middle Pleistocene alluvial fan deposits of the Mercure basin; 3) Middle-Pleistocene lacustrine deposits; 4) Lower Pleistocene slope and alluvial fan deposits; 5) Cretaceous to Oligocene ophiolite-bearing internal units; 6) Mesozoic-Cenozoic shallow-water carbonates; 7) Main faults; 8) Contour line.

planation surfaces, which are arranged in several superimposed levels located at higher altitudes above the infill of tectonic basins as a result of regional uplift, block-faulting, and fluvial incision. The axial sector of the chain underwent significant uplift during the Quaternary, with average rates of about 0.6 mm/yr. Quaternary uplift was attributed to thermal/isostatic regional raising coupled with local activity of high-angle faults (Schiattarella et al., 2017 and references therein). From a climate viewpoint, the southern Apennines chain is featured by a Mediterranean-type climate with dry summers, cold winters and a mean annual rainfall lower than 1,000 mm/yr. Heavier rainfall events are mainly concentrated in autumn and spring seasons. Recent trends highlight a general decrease in the total annual rainfall and an increase in dry periods and short-term extreme events (Piccarreta et al., 2013). Our knowledge about changes in precipitation and temperature pattern during Quaternary glacial stages is rather limited. Relict glacial landforms along the higher peaks (i.e., above an altitude of 1,800 m) of the Pollino Mts have been recognized (Giraudi, 2004) whereas indirect information at a regional scale from paleoclimate proxies suggest an increase of total precipitation and a drastic drop (at least 5°–6°) of the mean annual temperature (Baroni et al., 2018; McGee, 2020).

The Mercure basin is a tectonic depression of the axial zone of the southern Apennines, Italy, bordered to the west and east by the Mesozoic carbonate ridges of Lauria Mts and Mt. Pollino and filled mainly by Middle Pleistocene conglomerates and coeval clay and marls of fluvio-lacustrine environment (Figure 2). Similarly to other intermontane basins of the axial zone of the southern Apennines, Quaternary evolution of the Mercure basin was dominated by the activity of high-angle WNW-ESE-trending fault systems, which created the tectonic low where Middle Pleistocene lacustrine deposition occurred. The genesis and evolution of the endorheic depression are related to the reactivation with normal and oblique kinematics of a pre-existing N120°-trending strike-slip fault system (Schiattarella et al., 1994; Schiattarella et al., 2006). Left-lateral strike-slip N120°-trending fault zone and coeval NE-SW normal faults are responsible for the creation of an embryonal tectonic low (shaped as a counter-Apennine half-graben), which is characterized by the deposition of lower Pleistocene slope and alluvial fan sediments. The Middle Pleistocene reactivation of the older fault system (Castelluccio-Viggianello fault in Figure 2) in a NE-SW extensional stress field (Schiattarella et al., 1994; Gioia and Schiattarella, 2006; Brozzetti et al., 2009) promoted the relative uplift of the N110-120° trending la Fagosa ridge (northern border of the basin) and the development of the endorheic conditions. The lacustrine deposition ceased in the initial part of the Middle Pleistocene after the dissection of the Laino Borgo threshold by the Mercure-Lao River. The chronology of the lacustrine stage of the Mercure basin succession was recently constrained by $^{40}Ar/^{39}Ar$ age of two tephra layers cropping out in the south-eastern sector of the basin, not far from the top of the lacustrine deposits. Tephrocronological data indicate an age of 516 ± 3 ka and 493 ± 3 ka, which allowed to assign to the MIS13 the final stage of lacustrine deposition of the study area. On the

basis of the geochronological data (Giaccio et al., 2014), pollen analysis (Petrosino et al., 2014) and morpho-stratigraphic consideration, the timing of genesis, evolution and extinction of the endorheic phase of the basin was chronologically constrained between 0.7 and 0.5 My (Robustelli et al., 2014).

In the latest decades, the study area has been affected by two moderate to strong seismic events (the 9th September 1998 Mw 5.6 Mercure earthquake and the 26th October 2012 Mw 5.0 Mormanno earthquake, Brozzetti et al., 2017), with epicentres located along the northern and south-eastern basin-border slopes, respectively.

3 Methods

In the last two decades, modern morphotectonic studies frequently adopted approaches where traditional geomorphological analyses based on the field-based recognition of geomorphic markers of uplift/deformation are integrated by DEM analysis and extraction of quantitative parameters of topography and drainage network. In particular, river profile analysis aimed at the recognition of knickpoints/knickzones and/or modeling of transient reaches of longitudinal profiles of non-equilibrium channels have been used as one of the most effective methods to reconstruct fluvial response to active tectonics (Kirby and Whipple, 2012; Pavano et al., 2016), tectonic uplift (Schoenbohm et al., 2004; Schmidt et al., 2015), fault activity (Miller et al., 2013; Boulton, 2020) and changes in base-level (Harkins et al., 2007; Castillo et al., 2013; Struth et al., 2019). In this work, we combine river profile analysis, extraction of swath profiles, and analysis of the spatial distribution of geomorphic markers of basin evolution for the reconstruction of post-lacustrine evolution of the drainage net of the Mercure tectonic basin. Extraction of swath profiles and river longitudinal profiles is supported by the processing of a DEM with a spatial resolution of 5 m, which has been derived by the integration of LIDAR data and topographic maps. LIDAR-derived DEM was acquired by an airborne survey in 2013 and is available on the geoportal of the Basilicata Regional Authority (http://rsdi.regione.basilicata.it). Southernmost sectors of the study area are not covered by LIDAR survey: in this sector, altitude data were extracted by using contours and height points deriving from digital maps at a 1: 5,000 scale.

3.1 Morphotectonic analyses: Distribution of erosional surfaces, fluvio-lacustrine terraces and morpho-lineaments

Classical morphotectonic analyses are based on the identification and mapping of morphotectonic markers of ancient stages of basin evolution such as erosional land surfaces and fluvio-lacustrine terraces. Such geomorphic markers are crucial to retrace the long-term evolution of the study area, which is featured by complex interaction among regional uplift, fault activity, and climate-controlled base-level changes. Moreover, we also focused on the individuation of drainage network anomalies (i.e., right-angle confluences and fluvial elbows), which can provide additional information about the tectonic control on local-scale drainage basin evolution.

3.2 Swath profiles

Extraction of maximum, minimum and mean altitude and local relief into a predefined strip is a consolidated method to capture: i) Mean topographic features of a landscape; ii) the distribution of low-relief surfaces and iii) the amount of fluvial incision. We have extracted two profiles with a 1,000 m-wide swath along two main orientations using the SwathProfiler tool (Pérez-Peña et al., 2017). Profile 1–1′ roughly follows the course of the Mercure-Lao River along a NE-SW direction and extends northward to the border ridges of the basin whereas profile 2–2′ cut the study area across a roughly NW-SE orientation from the range of Pollino Mts to the Monti di Lauria ridges.

3.3 River profile analysis

The analysis of longitudinal river profiles using the stream power erosion model is one of the most powerful tools to investigate the complex interactions among climate, tectonics and topography and the long-term response of the fluvial net to the spatial and temporal distribution of uplift and erosion rates (Schoenbohm et al., 2004; Gioia et al., 2014; Ellis et al., 2015; Wang et al., 2017; Li et al., 2020). River profile analysis was carried out according to the methods and procedures developed by Wobus et al. (2006) using a 5 m DEM. Channel elevations and upstream drainage areas of 27 channels of the study area were extracted from a suite of MATLAB scripts (Forte and Whipple, 2019).

Empirical power-law between slope and area can be described as follow:

$$S = K_s A^{-\theta} \tag{1}$$

where S is slope, or channel gradient, k_s is the channel steepness index, A is the upstream contributing drainage area, and θ is the channel concavity index. The linear regression in log-log space to the slope–area data allows us to derive the concavity index (the slope of the regression, Whipple and Tucker, 1999) and the steepness index (the *y*-intercept, that is the projection of the best-fit line that intersects the *y*-axis, Whipple and Tucker, 1999). In transient landscapes, river profiles are frequently featured by different segments with a linear trend separated by knickpoints or knickzones (Kirby and Whipple, 2012). In these cases, it can be useful to calculate the channel slopes using the Chi gradient, an alternative estimation that introduces a reference drainage area and a Chi vs. elevation plot (Perron and Royden, 2013). To estimate the Chi value, we used the following equation:

$$\chi = \int_{xb}^{x} \left(\frac{A_0}{A(x)} \right)^{\frac{m}{n}} dx \tag{2}$$

where A_0 is the reference drainage (1 m^2) and m/n the concavity index (Perron and Royden, 2013). Such a representation allows easier identification of segments of the river profiles in a steady-state condition, which show a linear trend in the chi plot and a slope of the regression line proportional to the ratio U/K (i.e., rock uplift rate, U and rock resistance to erosion, K, a variable that incorporates both process- and bedrock-dependent variables, Whipple, 2004). Following this procedure, we have extracted the river longitudinal profiles of the main channels of the study area (i.e., about 27 tributaries of the Mercure River), identifying the knickpoints that are related to the different stages of morpho-evolution of the study area. Such data have

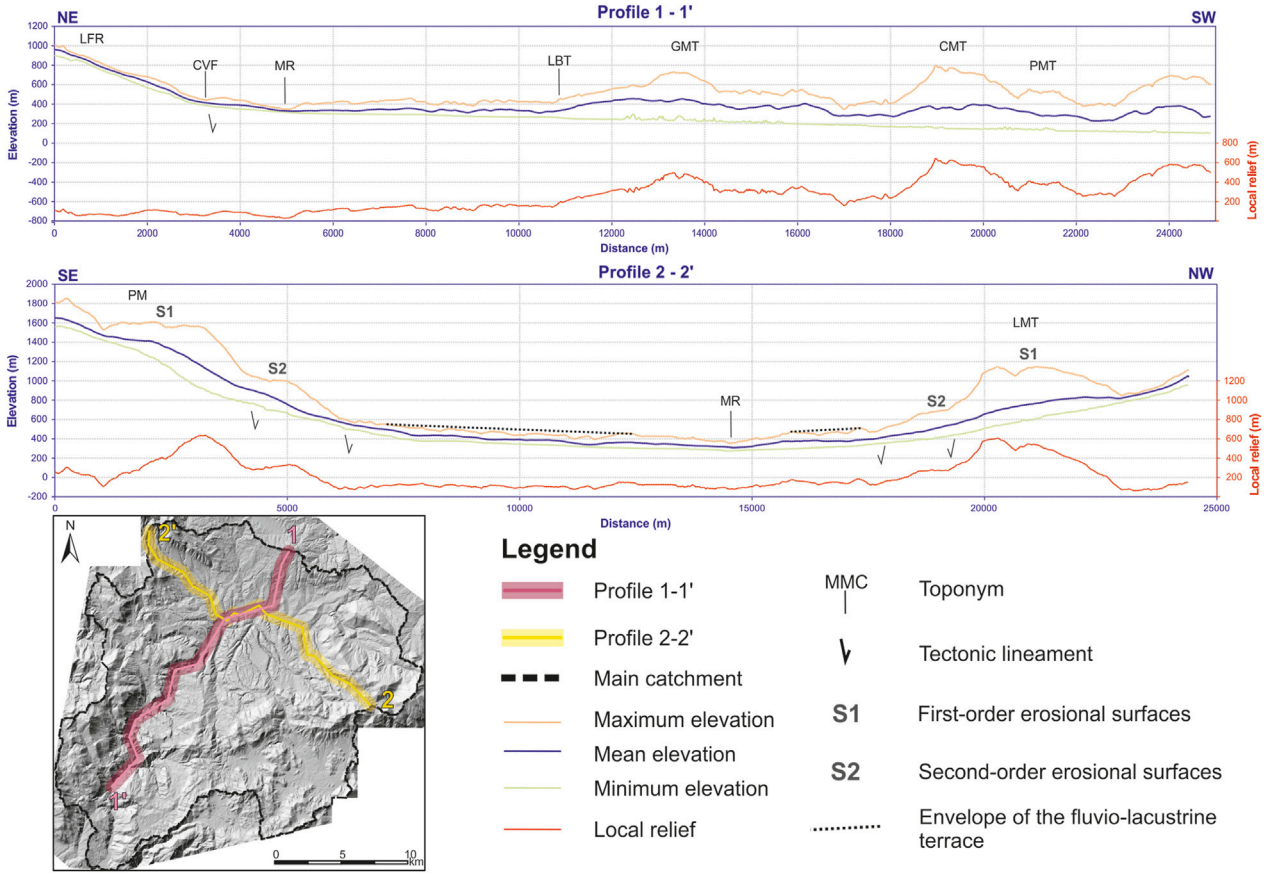

FIGURE 3
Topographic swath profiles (swath width: 1,000 m) crossing the Mercure River basin. Acronyms: LFR, la Fagosa ridge; CVF, Castelluccio-Viggianello fault; MR, Mercure River; LBT, Laino Borgo threshold; GMT, Gada Mts; CMT, Ciagola Mts; PMT, Papasidero-Mormanno Mts; PM, Pollino Massif; LMT, Lauria Mts.

been combined with the morphotectonic analysis and the spatial distribution of drainage network anomalies. Spatial and altimetric arrangements of knickpoints and knickzones have been compared with both lithological contrasts and altitude of morphotectonic markers of ancient base–levels (i.e., erosional land surfaces and fluvial terraces) in order to identify the anomalies related to base-level changes and tectonic processes. Moreover, local-scale disequilibrium state of the drainage basin has been investigated by combining field evidence with contrasts in values of several metrics such as chi, relief, and channel gradient along the water divides. Such an approach allowed us to infer spatial distribution of fluvial capture phenomena that strongly modified the drainage basin area after the cessation of the lacustrine deposition of the Mercure basin. Then, their spatial distribution has been used to infer: i) The palaeodrainage of the endorheic stage; ii) timing and amount of river incision of the post-lacustrine stage. Finally, a map of the normalized steepness index (ksn) and a Chi map were also determined for the study area using a best-fit reference concavity index of θ_{ref}= 0.35. This kind of estimation provides additional information about spatial distribution of perturbations induced by tectonic and climate forcing and changes in drainage basin area (Kirby and Whipple, 2012; Forte and Whipple, 2018; Struth et al., 2019). In particular, the Chi-map (Willett et al., 2014) furnished useful information about the degree of disequilibrium across water divides. Higher differences in Chi values across the drainage divides can be useful to identify channels with aggressive (*sensu* Forte and Whipple 2018, lower Chi values) and victim patterns (higher values of Chi) and consequently the location of drainage divide sectors affected or prone to capture phenomena (Willett et al., 2014).

4 Results

4.1 Topographic analysis

Swath profiles (Figure 3) provided first-order information about the fault-related relief growth and incision signal of the study area. In profile 1–1′, the highest values of the mean elevation correspond to the la Fagosa ridge, uplifted by the basin-border fault of the northern sector of the study area. Local relief between the Mercure River and Laino Borgo threshold (LBT in Figure 3) gave the amount of incision of the post-lacustrine stage of the basin evolution, which reached a value of about 140–150 m in the depocentral zone of the basin. In this sector, maximum elevation values are lower than those in the proximity of the Castelluccio-Viggianello fault. The highest values of the local relief can be observed in the southernmost sectors of the swath profile, where Mercure-Lao River deeply dissects the Ciagola-

10.3389/feart.2023.1112067

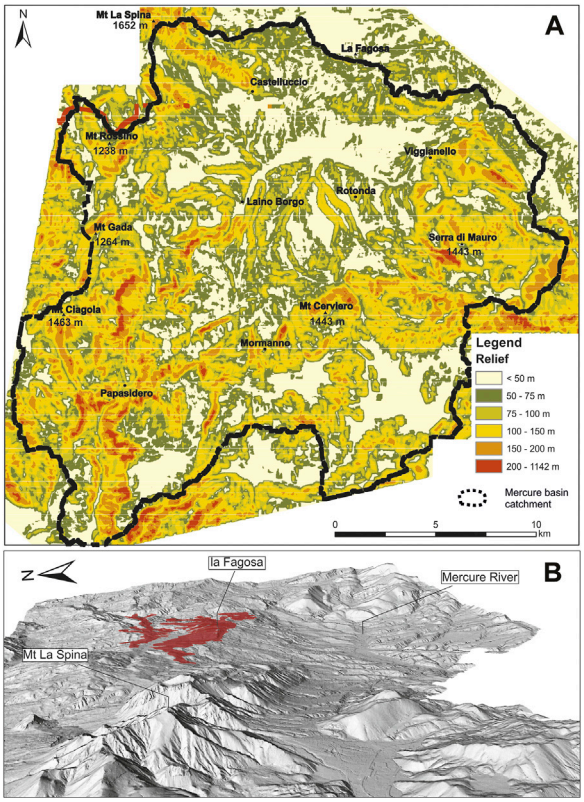

FIGURE 4
(A) Relief map of the study area (size of the moving windows: 200 m). Low-relief sectors at higher altitudes along the carbonate ridges roughly coincide with the remnants of the erosional surfaces whereas fault slopes are mainly represented by alignments of high relief areas. **(B)** View to the east of the low-relief palaeolandscape located along the top of the la Fagosa ridge. Note the north-eastern gentle dip toward the valley of the Sinni River of the erosional surface remnants.

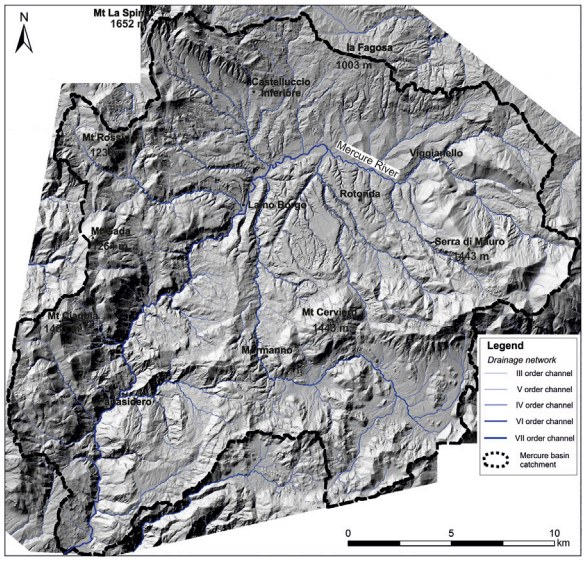

FIGURE 5
Catchment and drainage network of the Mercure River basin draped over the hillshade of the study area. Hierachization of the drainage net follows the Strahler's scheme.

Gada Mts and Mormanno-Papasidero carbonate highs. Profile 2–2′ shows the impressive relief of the basin borders with alternating low-relief landscapes and deep fluvial incisions. Fault slopes of the Pollino and Lauria ridges and erosional surfaces of the pre-lacustrine stages are also evident. In the middle sector of the profile, we can observe the gently-dipping geometry of the fluvio-lacustrine terraces, as inferred by the envelope of the maximum elevations directed toward the lowest sectors of the basin.

4.2 Spatial distribution of morphotectonic markers of ancient base-levels

The polyphase evolution of the study area promoted the development of relict landscapes and/or low-relief erosional surfaces that occurred in a staircase arrangement at the top of the landscapes or at higher altitudes than the basin infill (Figures 3, 4). The highest order of such geomorphic elements is represented by the remnants of an ancient flat landscape (summit palaeosurface, or S1 after Schiattarella et al. (2003)) strongly dislocated and scattered by block-faulting, generally found up to 1,300 m. Regional remarks about the relative age of the summit palaeosurface suggest that it developed in the Late Pliocene and its remnants were affected by diachronous stages of planation, erosion and tectonic dislocation during the initial part of the Early Pleistocene (Schiattarella et al., 2013). Another group of erosional land surfaces can be observed moving downward along the fault slopes of the Pollino and Lauria Mts. The remnants of such erosional surfaces occurred at the base of a first generation of fault slopes, which exhibit typical features of mature geomorphological elements. The remnants of S2 erosional land surfaces at lower altitudes are distributed along a narrower cluster of altitudes ranging from 700 to 850 m a.s.l. and are locally associated with slope and alluvial fan deposits, Lower Pleistocene in age. The widest remnant can be recognized along the top of la Fagosa ridge (Figure 4B), where it shows clear evidence of a relict landscape connected to a palaeodrainage oriented toward north-eastern sectors (i.e., toward the Sant'Arcangelo basin, a wide Pliocene to Pleistocene basin connected to the embryonal Mercure basin before the uplift of the la Fagosa ridge). Impressive and steeper fault slopes separated the S2 erosional surfaces from the fluvio-lacustrine terraces of the Mercure basin. The creation of the accommodation space for the deposition of the thick basin infill was related to an important tectonic phase of block-faulting along N120°-trending normal faults, which occurred in the final part of the Lower Pleistocene. This phase was later accompanied by gentle tilting towards the NE, as shown by the north-eastern dip and drag of the lacustrine deposits outcropping along the northern sector of the basin.

4.3 River profile analysis

Analysis of the longitudinal profiles of the Mercure River and its major tributaries (Figure 5) was carried on 27 tributaries of the Mercure River (See Supplementary Material for additional details about the interpretation of the river profiles). Our study reveals a

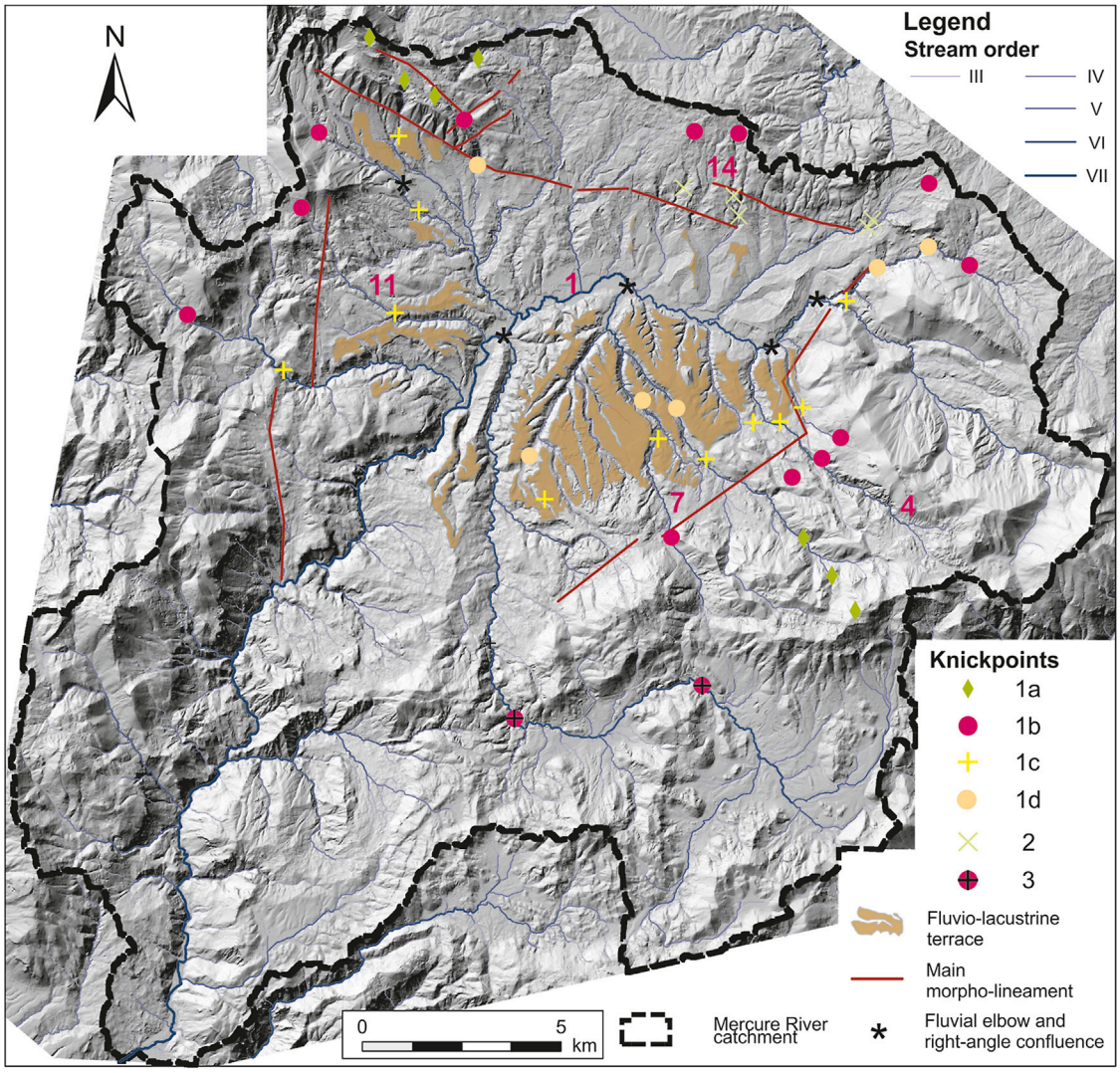

FIGURE 6
Morphotectonic map of the study area showing knickpoint distribution, fluvio-lacustrine terraces, and the main morpho-lineaments. Legend: 1a, 1b, 1c, 1d: knickpoint related to the base-level falls; 2) end of knickzone related to the activity of the Castelluccio-Viggianello fault; 3) knickpoint related to fluvial capture phenomena. Numbers in red indicate the location of channels investigated in Panel 6.

shape of the profiles that strongly deviates from the concave or equilibrium form of the elevation-distance plot, being recognizable knickpoints/knickzones related to different genesis mechanisms. Each of these segments has been classified in relation to the main genetic processes by comparing their distribution with lithologic contrasts, local-scale tectonic disturbance and altitude of morphotectonic markers of ancient base–levels (i.e., erosional land surfaces and fluvio-lacustrine terraces). Such an approach allowed us to group the main knickpoints of the study area in three categories (Figure 6), which are attributed to the perturbation responsible for their development and migration (i.e., base-level fall, faulting, and fluvial capture, Figure 6). Knickpoints related to past ancient base-levels are the most represented in the longitudinal profiles of the study area. They are located within narrow altitude ranges and generally separate segments of the profiles with similar features in terms of steepness and concavity indexes. Moreover, they have a low-relief surface along the valley flanks and can be related to ancient base-levels and interpreted as the results of upward migration of the incision wave induced by tectonic and climatic changes in base-levels. In this group of knickpoints, we recognized three different orders of knickpoints ranging in altitude from 1,715 to 430 m a.s.l. (Figure 6), which have been correlated to the correspondent genetic mechanisms/relict landscape orders and isolated segments with a similar gradient in the chi plot. In particular, knickpoints related to the lacustrine stage of the study area are well recognizable, especially in the south-eastern and north-western sectors of the study area (see for example rivers 4, 7 and 11 in Figure 7). They depicted the plano-altimetric distribution of the palaeodrainage during the lacustrine stage of the basin and are distributed between 595 and 465 m a.s.l.: in this cluster of knickpoints, lower altitudes occurred in river profiles of the western sectors of the basin (i.e., Fosso Mangosa, Canale della Canica and Fosso Jannello rivers, Figure 6) whereas longitudinal profiles of the channels flowing into the south-eastern sectors of the study area show a narrower range of altitude distribution of

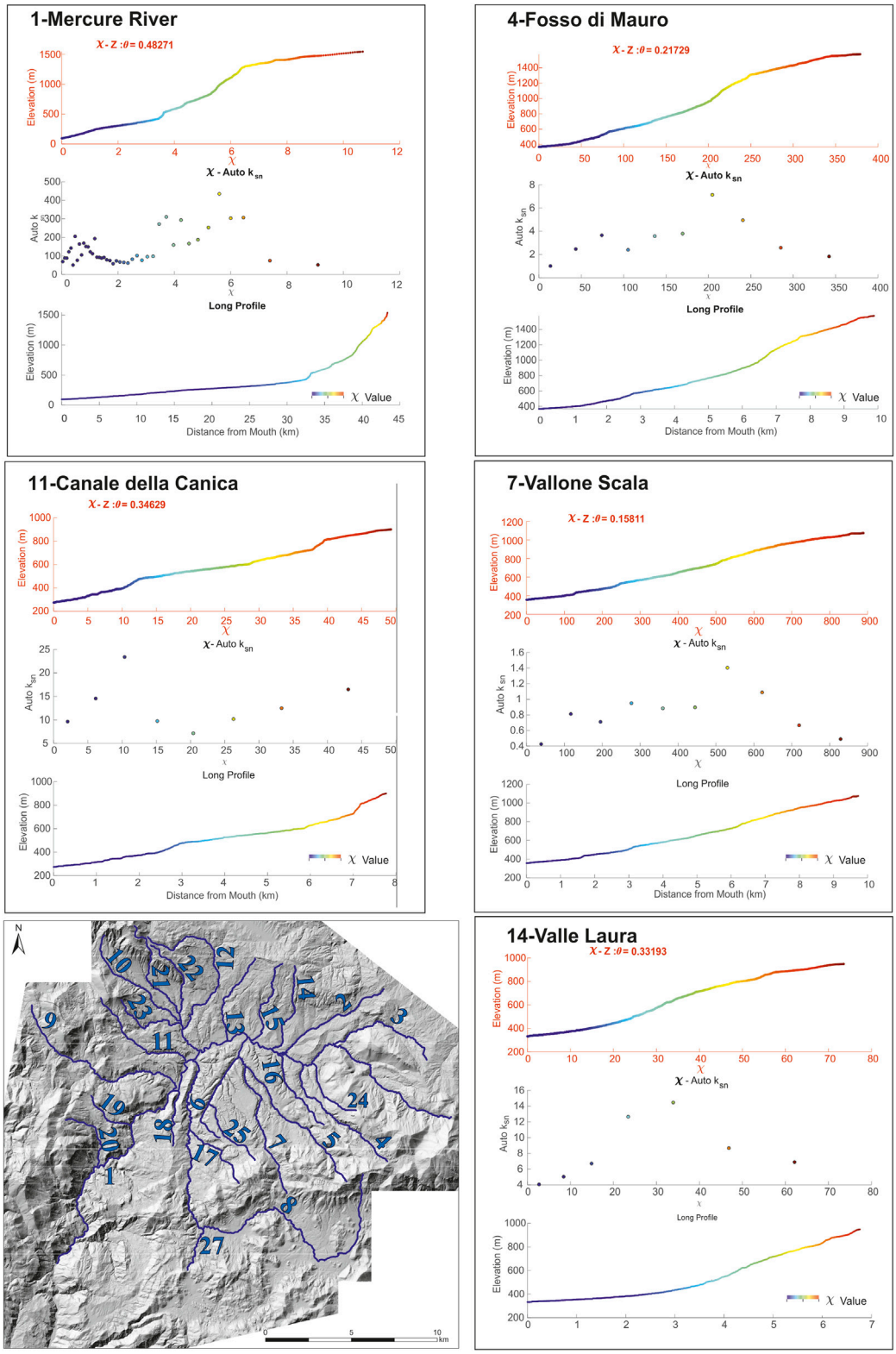

FIGURE 7
Examples of representative longitudinal profiles of the Mercure River basin. Numbering in the map shows the tributaries modelled by river profile analysis: 1: Mercure River, 2: Fosso Turbolo, 3: Fosso Torno, 4: Fosso di Mauro, 5: Fosso Paraturo, 6: Fosso Schettino, 7: Vallone Scala, 8: Fosso Battendiero, 9: Fosso Jannello, 10: Fosso Mangosa; 11: Canale della Canica, 12: Fosso del Pegno; 13: Fosso del Feto; 14: Valle Laura; 15: Valle Truscera; 16: Fosso di Grottascura; 17: Torrente Incugnatore; 18: il Canale; 19: Fosso della Montagna; 20: Fosso Gammio; 21: Fosso Magliasole; 22: Fosso San Giovanni; 23: Fosso di Castelluccio; 24: Vallone Zifero: 25: Fosso di Carlomagno; 26: Fosso Jannace; 27: Vallone Gavaretto.

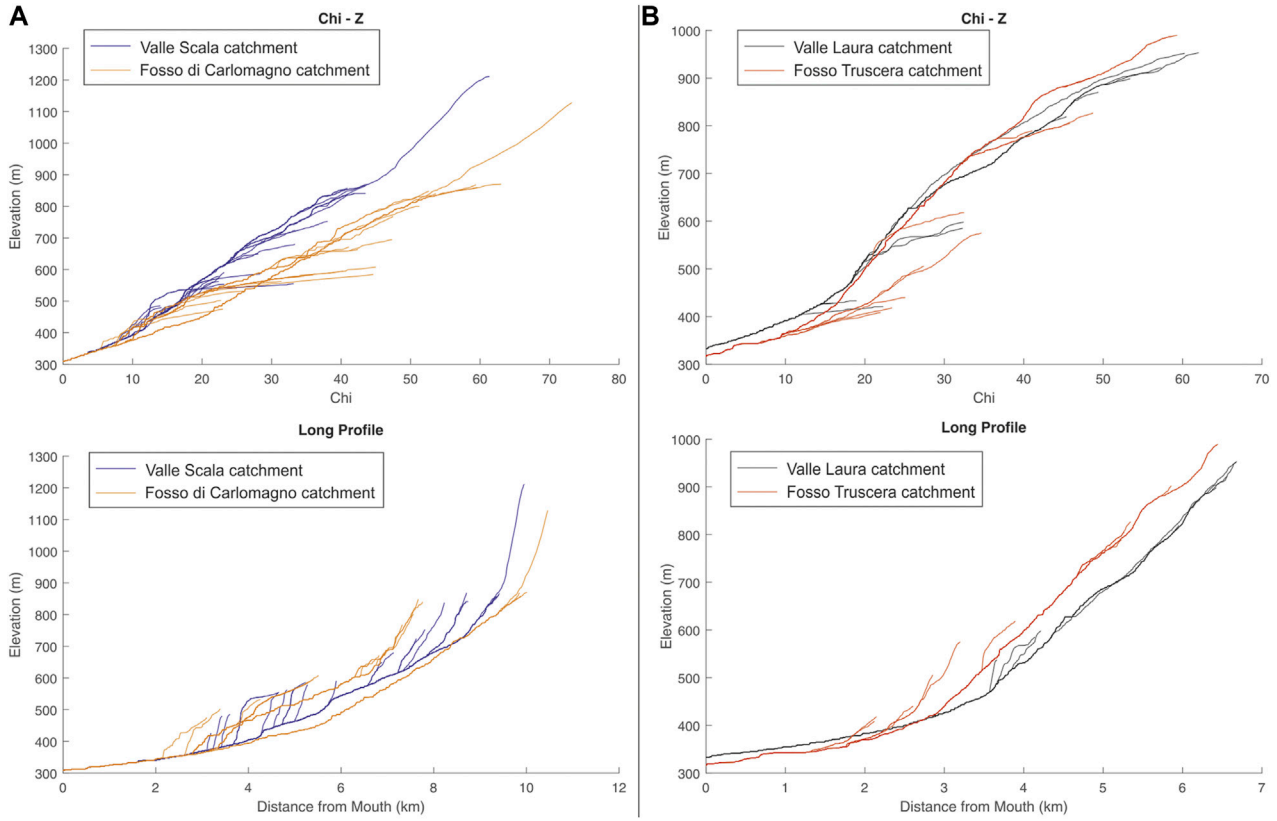

FIGURE 8
Comparison between river profiles and chi plots for two catchments located in southern **(A)** and northern **(B)** sectors of the study area.

knickpoints (i.e., from 540 to 595 m a.s.l.). Other knickpoints at about 400 m a.s.l. can be discriminated in some cases, as for example that of the Vallone Scala stream (Figures 6, 7).

Longitudinal profiles located along the northern sector of the study area homogeneously exhibit different features than the previous ones (Figure 8) due to the presence of a prominent concave-up shape in the vicinity of the trace of the Castelluccio-Viggianello fault (see for example river 14 in Figure 7). Such evidence together with those deriving from the anomalous high values of the normalized channel steepness index and the spatial distribution of several morphotectonic evidence (i.e., fault scarps and wine-glass valleys in erodible rocks such as the shaly rocks of the Ligurian accretionary complex) permitted reconstructing the trace of the fault system in the northern sector of the Mercure basin (Figure 6). Knickzones and channel steepening near the faults can be attributed to the transient response of the fluvial system to the fault activity. They can be classified as slope-break knickpoint (sensu Kirby and Whipple, 2012) and are preferentially aligned along a NW-SE orientation. Longitudinal profiles of the channels located along the northern sector of the basin are also featured by prominent knickpoints related to the palaeodrainage of the embryonal Mercure basin, which pre-dates the fault-related uplift of the la Fagosa ridge responsible for the development of endorheic condition of the Mercure basin.

Finally, other knickpoints with different features than the previous ones are clustered in the upper and mid reach of the catchment of the Battendiero Fosso River. Visual inspection of the Chi map (Figure 9) suggests that the channels in the right-orographic side of the Battendiero River have lower Chi values than those of the easternmost sectors and a marked Chi contrast across the divides was also detected (Figure 9). Such data, together with a pronounced inflection of the drainage divide, indicate a large-scale aggressor role for the channels of the Battendiero catchment and an eastward drainage migration during the incision wave related to the post-lacustrine stage. A Chi contrast is found also along the divide between the Torrente Incugnatore and the Fosso di Carlomagno catchments. Higher values in the former suggest a trend of divide migration towards the east as well.

4.4 Rates of fluvial incision and knickpoint migration

Estimations of the incision rate of the Mercure River and its tributaries were performed by comparing the altitude difference between the projected equilibrium profiles of the lacustrine stage and the present-day form of the longitudinal profiles (Figure 10). A robust value of the rate of vertical incision and knickpoint migration related to the endorheic-exorheic transition can be provided by the well-constrained timing of the end of the lacustrine deposition in the Pleistocene half-graben.

The longitudinal profile of the Mercure River (Figure 7) is characterized by two clear knickpoints that separate three segments of the profile with different values of steepness and concavity indexes: an upper segment that crossed over the low-

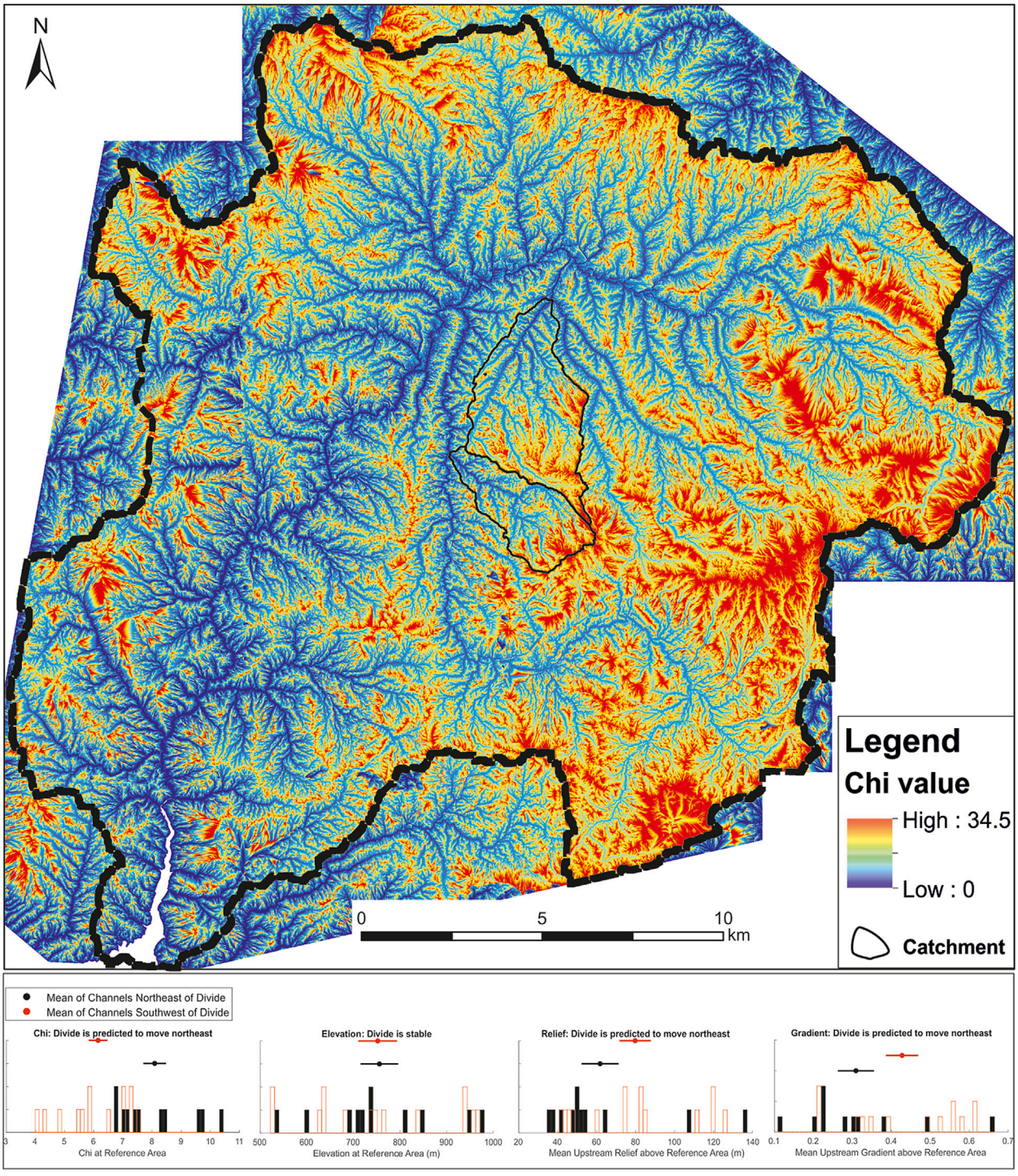

FIGURE 9
Chi map of the Mercure River basin and divide metric histograms for the Torrente Incugnatore and Fosso di Carlomagno catchments. Note the higher difference of Chi values along the divide of the two catchments.

relief relict landscapes of the Mesozoic carbonate ridges with a uniform concavity index and low steepness index, a middle segment with high concavity and steepness indexes, and a lower channel segment with intermediate concavity and steepness indexes. The middle segment highlights a more complex geometry with several knickpoints at altitudes comparable with those of both S2 erosional surfaces and fluvio-lacustrine terraces. The main knickpoint of the profile is located at about 530 m a.s.l. and it roughly corresponds to the altitude of the dissected threshold of the palaeolake inferred from morphotectonic markers. The projection of the palaeoprofile of the Mercure River related to the lacustrine stage of the basin (i.e., the segment of the longitudinal

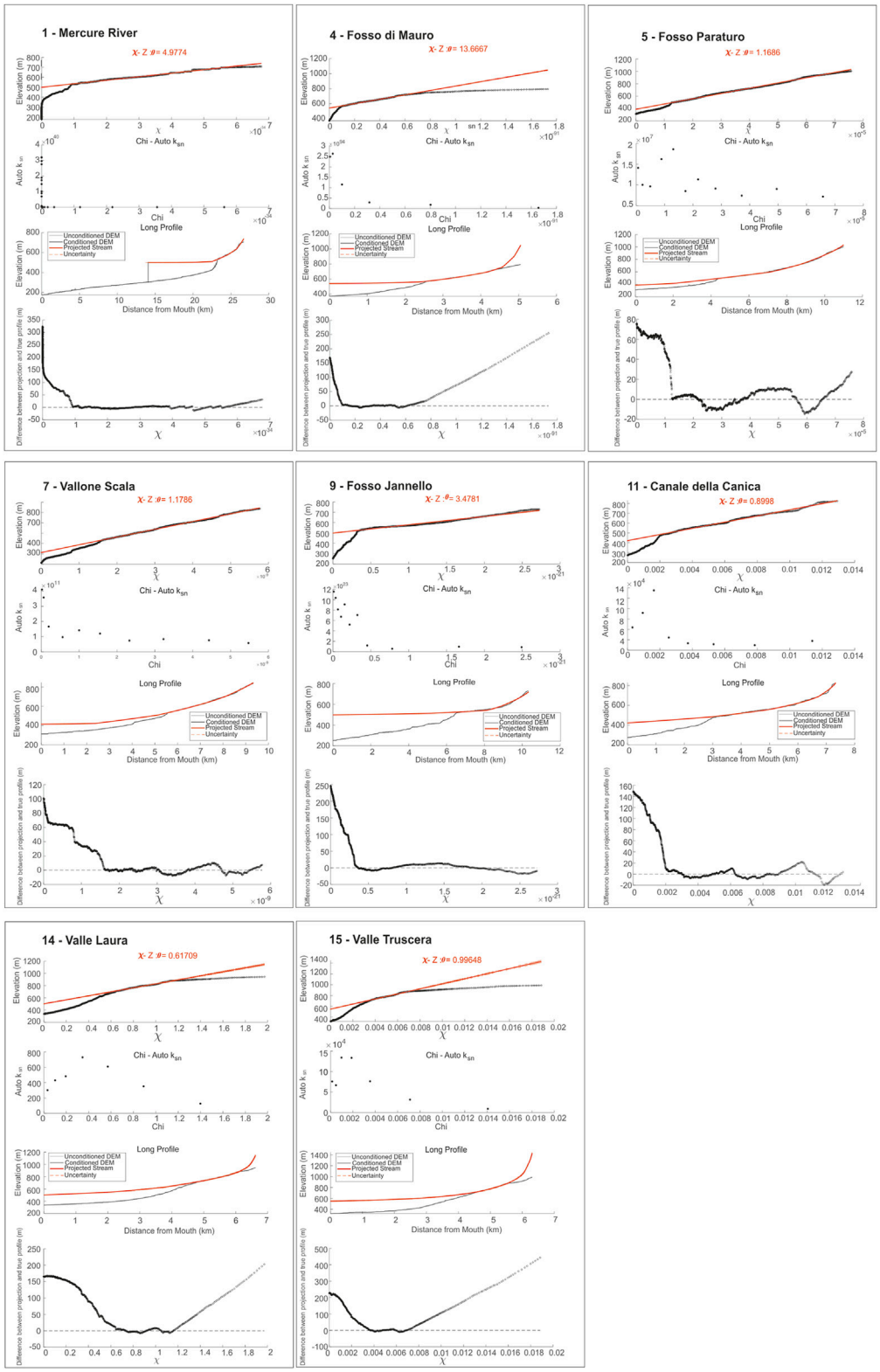

FIGURE 10
Reconstruction of the incision depth from transient segments of selected channels of the study area.

profile comprised between the base of the S2-related knickpoint and the knickpoint at 530 m a.s.l., see Figure 10) provides a value of ca. 150 m of the amount of fluvial incision induced by the endorheic-exorheic transition of the basin. Assuming that the erosion of the threshold of the Mercure lake occurred during the base-level fall of the MIS 12, the estimated mean incision rate is about 0.35 mm/yr

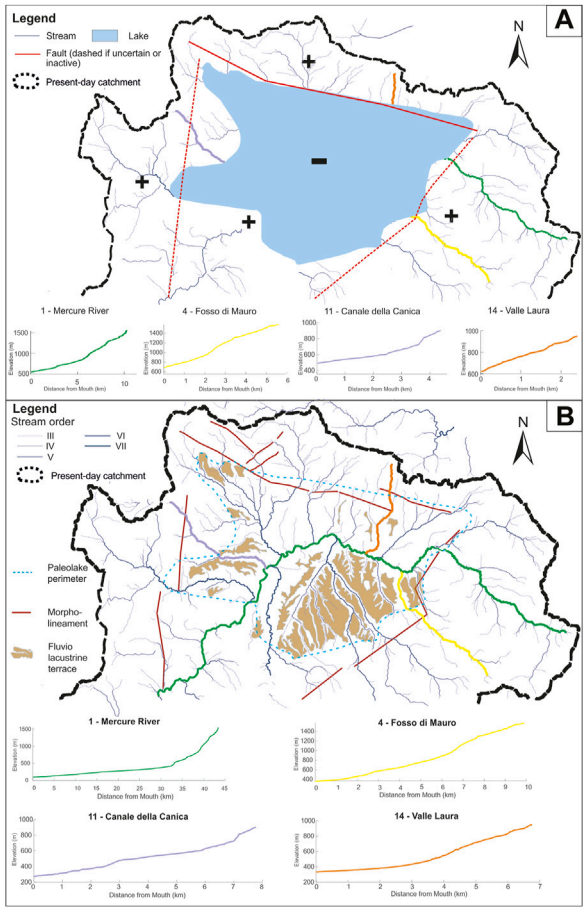

FIGURE 11
Sketch showing the drainage network evolution of the study area (see text for further explanation). **(A)** Schematic reconstruction of the drainage network pattern and longitudinal profiles prior to the drainage integration; **(B)** present-day landscape.

while the rate of knickpoint migration reached values of several tens of meters for years. Yet, it is possible that vertical incision slowed down during the rising of the eustatic curve during the MIS 11, so permitting the formation of the knickpoints at about 400 m a.s.l. due to the successive sea-level (or local base-level) fall. The amount of incision of the tributaries ranges from about 80 m in the Torrente Paraturo river to about 140 m in the Fosso di Mauro and Canale della Canica rivers (Figure 10).

Following the same approach, we reconstruct the paleoprofiles of the channels located in the northern sector of the basin. The projection of the knickzones related to the differential uplift induced by the border fault of the basin (Castelluccio-Viggianello fault) can provide an estimation of the fault throw since the Early-Middle Pleistocene. In particular, the reconstruction of the vertical offset between the projected concave-up transient segments of the longitudinal profiles and the present-day thalwegs of Valle Laura and Fosso Truscera rivers highlights a maximum value of about 200 m. The vertical offset of about 140 m can furnish information about the footwall uplift of the la Fagosa ridge, which occurred at the end of the Early Pleistocene (i.e., after both the deposition of Lower Pleistocene slope and alluvial fan deposits and the formation of the S2 relict palaeolandscape occurring at the top of la Fagosa ridge). Assuming that the start of the knickpoint development coincides with the morphotectonic stage of fault-related uplift of la Fagosa ridge and the coeval creation of the endorheic condition, the minimum slip rate of the fault is about 0.7 mm/yr.

5 Discussion

The morphotectonic evolution of the study area is mainly controlled by poly-kinematics high-angle WNW-ESE and NE-SW oriented faults, which promoted the development of a complex landscape with low-relief relict erosional surfaces that produced a staircase arrangement at higher altitudes than the basin infill top. The two stages of creation and delineation of the Mercure basin are well recorded by channel profile forms, which exhibit clear knickpoints at altitudes comparable with those of the superimposed landscapes related to both the initial formation of the tectonic low and the evolution of the endorheic basin. Thus, a modern river profile analysis can be a valuable tool to reconstruct the evolution of transient landscapes where classical morphotectonic markers of long-term evolution are ambiguous or dismantled by erosion processes.

Longitudinal river profiles of the study area record the long-term morphotectonic evolution of the Mercure tectonic basin, highlighting a transient state of the fluvial system with clear knickpoints and knickzones related to relict landscapes or Quaternary activity of high-angle faults. In particular, the knickpoints related to the lacustrine stage (Figure 11), well preserved in channels of the south-eastern and north-western sectors of the basin, were used as geomorphic markers to estimate rates of fluvial entrenchment. Also the knickpoint migration due to the incision wave, in turn induced by tectonic and climatic changes in base-levels, were estimated.

The well-constrained timing of endorheic-exorheic transition provides an uncommon opportunity to: i) investigate the complex relationships among tectonic, climate, and drainage network re-organization; ii) estimate rates of fluvial incision and knickpoint migration induced by dramatic base-level fall. The projection of the palaeoprofile of the Mercure River related to the lacustrine stage of the basin (Figure 10) provides a value of about 150 m of fluvial incision induced by endorheic-exorheic transition of the Mercure basin and a mean incision rate of about 0.35 mm/yr. Concerning the mechanism of drainage integration, the timing of lake extinction suggests a relevant role of the eustatic drop of the MIS 12, which certainly favored a headward propagation of an incision pulse of the drainage system located to the SW of the lake threshold (Figure 11A). On the other hand, plano-altimetric distribution of lacustrine deposits in the threshold sector indicates a possible role of lake spillover. Such an interpretation was also proposed by Robustelli et al. (2014) on the basis of facies analysis and morphostratigraphic correlation.

Comparison with uplift rates from other areas of the axial zone of southern Apennines suggests that the incision rates of the Mercure River basin during the Middle Pleistocene are lower than other areas of the chain with a similar morphotectonic evolution. More specifically, an average value of incision rates of ca 0.6 mm/yr can be reconstructed by morphotectonic markers in other sectors of the axial zone of the chain (see for example Schiattarella et al., 2017). Differential movements along the

Castelluccio-Viggianello fault and more specifically the role of subsidence of the hanging-wall-in a context otherwise dominated by regional uplift-can explain the observed distribution of vertical movement. Alternatively, several morphotectonic evidences (i.e., morpho-stratigraphic relationships between late Quaternary alluvial terraces of the Mercure River and fluvio-lacustrine terraces and the presence of Upper Pleistocene slope deposits and alluvial fans that sealed the entrenched fluvial valleys) suggest that most of the vertical incision of the study area occurred during the pronounced eustatic base-level changes between MIS12 and MIS10. In this case, a higher value of ca 0.6 mm/yr of fluvial incision rates of the study area can be estimated.

Post-lacustrine geomorphological evolution of the Mercure basin strongly controls the morphometric features of the drainage network, which preserves a centripetal pattern with several planimetric anomalies such as counterflow and high-angle confluences (Figure 11B). One of the most evident anomalies is represented by the planimetric shape of the Battendiero Fosso River, which flow with a right angle in a roughly N-S direction toward a NNE-SSW reach of the Mercure River (Figure 5). Several geomorphic evidence (i.e., anomalous inflection of drainage divides and distribution of knickpoints related to capture phenomena) and the pattern of the Chi values in the right-orographic side and southernmost sectors of the Battendiero Fosso catchment suggest that its channels have largely extended their headwaters toward the south after the cessation of the lacustrine phase. In particular, morphometric analysis indicates an aggressive pattern of the channels located in the right-orographic side of that stream, which promoted an eastward migration of the divide with a significant decrease of the drainage area of the contiguous Fosso Carlomagno catchment.

Spatial distribution of knickpoints in river profiles of the northern sector of the study area suggests a strong influence of block-faulting on the landscape evolution of this sector of the Mercure basin. A well-developed concave-up segment in those profiles was recognized between an upward trait with lower values of channel steepness and the trace of the Castelluccio-Viggianello fault. Such morphometric features of the channels and the occurrence of several morphotectonic evidences such as small fault-related scarps and wineglass-shaped valleys in erodible shaly rocks of the Ligurian units represent the geomorphic response of the landforms to an increase in footwall uplift rate due to accelerated slip along the Castelluccio-Viggianello fault. Such a response is mainly due to the fault-related uplift of the la Fagosa ridge, promoting the development of endorheic condition of the Mercure basin.

6 Final remarks

Long-term response of a drainage system to the base-level fall induced by an endorheic/exorheic transition was investigated in the Mercure basin, a large intermontane basin of the axial zone of southern Apennines. Our results highlight that topographic analysis, drainage network morphometry, river profile analysis and spatial distribution of fluvio-lacustrine terraces can constrain the spatial and temporal pattern of base-level fall induced by tectonic and climate forcing of a complex transient landscape. Quaternary morphotectonic evolution of the study area strongly controls the channel profile forms, which exhibit clear knickpoints at different altitudes related to different genetic mechanisms. Knickpoints in river profiles of the north-western and south-east sectors are correlated to the base-level fall induced by the lake extinction. They have been used as geomorphic markers to estimate a rate of fluvial incision of ca 0.35 mm since the Middle Pleistocene. Post-lacustrine evolution of the drainage network is also featured by fluvial capture phenomena and drainage divide migration, which strongly modified the original pattern of fluvial net in the southern sector of the study area. The creation of the accommodation space for the deposition of the thick basin infill was related to an important tectonic phase of block-faulting along N120°-trending normal faults, which occurred in the final part of the Lower Pleistocene. Such an evolution promoted the formation of a concave-up segment in river profiles of these channels, which is useful to constrain the activity of the master fault of the basin. We confirm that river profiles are a powerful tool for reconstructing the spatial and temporal patterns of tectonic and climate forcing of complex landscapes, especially where other geologic/geomorphic methods provide contrasting information.

Data availability statement

The original contributions presented in the study are included in the article/Supplementary Material, further inquiries can be directed to the corresponding author.

Author contributions

DG contributed to conception and design of the study. DG, GC, AA, and MD performed the analysis. DG wrote the first draft of the manuscript. DG, GC, AA, and MS revised the draft and wrote the final version of the manuscript. All authors contributed to manuscript revision, read, and approved the submitted version.

Conflict of interest

The authors declare that the research was conducted in the absence of any commercial or financial relationships that could be construed as a potential conflict of interest.

Publisher's note

Supplementary material

The Supplementary Material for this article can be found online at: https://www.frontiersin.org/articles/10.3389/feart.2023.1112067/full#supplementary-material

References

Armstrong, I. P., Yanites, B. J., Mitchell, N., DeLisle, C., Douglas, B. J., and Valla, P. (2021). Quantifying normal fault evolution from river profile analysis in the northern basin and range province, southwest Montana, USA, *Lithosphere*, 2021, 1–25. doi:10.2113/2021/7866219

Aucelli, P. P. C., D'Argenio, B., Della Seta, M., Giano, S. I., and Schiattarella, M. (2014). Foreword: Intermontane basins: Quaternary morphoevolution of central-southern Italy. *Rendiconti Lincei* 25 (2), 107–110. doi:10.1007/s12210-014-0356-3

Baroni, C., Guidobaldi, G., Salvatore, M. C., Christl, M., and Ivy-Ochs, S. (2018). Last glacial maximum glaciers in the Northern Apennines reflect primarily the influence of southerly storm-tracks in the Western Mediterranean. *Quat. Sci. Rev.* 197, 352–367. doi:10.1016/j.quascirev.2018.07.003

Ben Moshe, L., Haviv, I., Enzel, Y., Zilberman, E., and Matmon, A. (2008). Incision of alluvial channels in response to a continuous base level fall: Field characterization, modeling, and validation along the Dead Sea. *Geomorphology* 93 (3-4), 524–536. doi:10.1016/j.geomorph.2007.03.014

Boulton, S. J. (2020). Geomorphic response to differential uplift: River long profiles and knickpoints from guadalcanal and makira (Solomon islands). *Front. Earth Sci.* 8 , 1–23. doi:10.3389/feart.2020.00010

Brozzetti, F., Cirillo, D., de Nardis, R., Cardinali, M., Lavecchia, G., Orecchio, B., et al. (2017). Newly identified active faults in the Pollino seismic gap, southern Italy, and their seismotectonic significance. *J. Struct. Geol.* 94, 13–31. doi:10.1016/j.jsg.2016.10.005

Brozzetti, F., Lavecchia, G., Mancini, G., Milana, G., and Cardinali, M. (2009). Analysis of the 9 september 1998 Mw 5.6 mercure earthquake sequence (southern Apennines, Italy): A multidisciplinary approach. *Tectonophysics* 476 (1-2), 210–225. doi:10.1016/j.tecto.2008.12.007

Castillo, M., Bishop, P., and Jansen, J. D. (2013). Knickpoint retreat and transient bedrock channel morphology triggered by base-level fall in small bedrock river catchments: The case of the Isle of Jura, Scotland. *Geomorphology* 180-181, 1–9. doi:10.1016/j.geomorph.2012.08.023

Cunha, P. P., Martins, A. A., Gomes, A., Stokes, M., Cabral, J., Lopes, F. C., et al. (2019). Mechanisms and age estimates of continental-scale endorheic to exorheic drainage transition: Douro River, Western Iberia. *Glob. Planet. Change* 181, 102985. doi:10.1016/j.gloplacha.2019.102985

Dorn, R. I., Skotnicki, S. J., Wittmann, A., and Van Soest, M. (2020). Provenance in drainage integration research: Case studies from the Phoenix metropolitan area, south-central Arizona. *Geomorphology* 371, 107430. doi:10.1016/j.geomorph.2020.107430

Ellis, M. A., Barnes, J. B., and Colgan, J. P. (2015). Geomorphic evidence for enhanced Pliocene-Quaternary faulting in the northwestern Basin and Range. *Lithosphere* 7 (1), 59–72. doi:10.1130/L401.1

Forte, A. M., and Whipple, K. X. (2018). Criteria and tools for determining drainage divide stability. *Earth Planet. Sci. Lett.* 493, 102–117. doi:10.1016/j.epsl.2018.04.026

Forte, A. M., and Whipple, K. X. (2019). Short communication: The topographic analysis kit (TAK) for TopoToolbox. *Earth Surf. Dynam.* 7 (1), 87–95. doi:10.5194/esurf-7-87-2019

Giaccio, B., Galli, P., Peronace, E., Arienzo, I., Nomade, S., Cavinato, G. P., et al. (2014). A 560-440 ka tephra record from the Mercure Basin, southern Italy: Volcanological and tephrostratigraphic implications. *J. Quat. Sci.* 29 (3), 232–248. doi:10.1002/jqs.2696

Giano, S. I., Gioia, D., and Schiattarella, M. (2014). Morphotectonic evolution of connected intermontane basins from the southern Apennines, Italy: The legacy of the pre-existing structurally controlled landscape. *Rendiconti Lincei* 25, 241–252. doi:10.1007/s12210-014-0325-x

Gioia, D., Gallicchio, S., Moretti, M., and Schiattarella, M. (2014). Landscape response to tectonic and climatic forcing in the foredeep of the southern Apennines, Italy: Insights from quaternary stratigraphy, quantitative geomorphic analysis, and denudation rate proxies. *Earth Surf. Process. Landforms* 39 (6), 814–835. doi:10.1002/Esp.3544

Gioia, D., and Schiattarella, M. (2006). Caratteri morfotettonici dell'area del Valico di Prestieri e dei Monti di Lauria (Appennino meridionale). *Il Quat.* 19, 129–142.

Gioia, D., Schiattarella, M., Mattei, M., and Nico, G. (2011). Quantitative morphotectonics of the Pliocene to quaternary Auletta basin, southern Italy. *Geomorphology* 134 (3-4), 326–343. doi:10.1016/j.geomorph.2011.07.009

Gioia, D., and Schiattarella, M. (2020). Modeling short-term landscape modification and sedimentary budget induced by dam removal: Insights from LEM application. *Appl. Sciences-Basel* 10 (21), 7697. doi:10.3390/App10217697

Giraudi, C. (2004). "The apennine glaciations in Italy," in *Quaternary Glaciations—Extent and Chronology, Part I: Europe*. Editors J. Ehlers and P. L. Gibbard (Amsterdam: Elsevier), 215223.

Gootee, B. F., Cook, J. P., Youberg, A., Douglass, J. C., Pearthree, P. A., and Heizler, M. T. (2022). Development and integration of the middle Gila River in the Safford basin, southeastern Arizona. *Geomorphology* 399, 108074. doi:10.1016/j.geomorph.2021.108074

Harkins, N., Kirby, E., Heimsath, A., Robinson, R., and Reiser, U. (2007). Transient fluvial incision in the headwaters of the Yellow River, northeastern Tibet, China. *J. Geophys. Res. Earth Surf.* 112 (3), F03S04. doi:10.1029/2006JF000570

Hilgendorf, Z., Wells, G., Larson, P. H., Millett, J., and Kohout, M. (2020). From basins to rivers: Understanding the revitalization and significance of top-down drainage integration mechanisms in drainage basin evolution. *Geomorphology* 352, 107020. doi:10.1016/j.geomorph.2019.107020

Kent, E., Boulton, S. J., Whittaker, A. C., Stewart, I. S., and Cihat Alçiçek, M. (2017). Normal fault growth and linkage in the Gediz (Alaşehir) Graben, Western Turkey, revealed by transient river long-profiles and slope-break knickpoints. *Earth Surf. Process. Landforms* 42 (5), 836–852. doi:10.1002/esp.4049

Kirby, E., and Whipple, K. X. (2012). Expression of active tectonics in erosional landscapes. *J. Struct. Geol.* 44, 54–75. doi:10.1016/j.jsg.2012.07.009

Larson, P. H., Dorn, R. I., Gootee, B. F., and Seong, Y. B. (2022). Drainage integration in extensional tectonic settings. *Geomorphology* 399, 108082. doi:10.1016/j.geomorph.2021.108082

Larson, P. H., Dorn, R. I., Skotnicki, S. J., Seong, Y. B., Jeong, A., and DePonty, J. (2020). Impact of drainage integration on basin geomorphology and landform evolution: A case study along the salt and verde rivers, sonoran desert, USA. *Geomorphology* 371, 107439. doi:10.1016/j.geomorph.2020.107439

Li, Q., Qin, B., and Pan, B. (2020). Bedrock channel width responses to tectonic uplift and lithologic resistance in the northern qilian mountains. *Quat. Sci.* 40 (1), 132–147. doi:10.11928/j.issn.1001-7410.2020.01.13

Marra, F. (1998). Evidence of late Pleistocene strike-slip tectonics at the calabria-lucania border: Structural and morphostratigraphic analysis of the Mercure basin. *Alp. Mediterr. Quat.* 11 (2), 201–215.

Marra, F., Frepoli, A., Gioia, D., Schiattarella, M., Tertulliani, A., Bini, M., et al. (2022). A morphotectonic approach to the study of earthquakes in Rome. *Nat. Hazards Earth Syst. Sci.* 22 (7), 2445–2457. doi:10.5194/nhess-22-2445-2022

McGee, D. (2020). Glacial-interglacial precipitation changes. *Ann. Rev. Mar. Sci.* 12, 525–557. doi:10.1146/annurev-marine-010419-010859

Menardi Noguera, A., and Rea, G. (2000). Deep structure of the campanian-lucanian arc (southern apennine, Italy). *Tectonophysics* 324, 239–265. doi:10.1016/s0040-1951(00)00137-2

Miller, S. R., Sak, P. B., Kirby, E., and Bierman, P. R. (2013). Neogene rejuvenation of central Appalachian topography: Evidence for differential rock uplift from stream profiles and erosion rates. *Earth Planet. Sci. Lett.* 369-370, 1–12. doi:10.1016/j.epsl.2013.04.007

Pavano, F., Pazzaglia, F. J., and Catalano, S. (2016). Knickpoints as geomorphic markers of active tectonics: A case study from northeastern sicily (southern Italy). *Lithosphere* 8 (6), 633–648. doi:10.1130/L577.1

Pérez-Peña, J. V., Al-Awabdeh, M., Azañón, J. M., Galve, J. P., Booth-Rea, G., and Notti, D. (2017). SwathProfiler and NProfiler: Two new ArcGIS Add-ins for the automatic extraction of swath and normalized river profiles. *Comput. Geosciences* 104, 135–150. doi:10.1016/j.cageo.2016.08.008

Perron, J. T., and Royden, L. (2013). An integral approach to bedrock river profile analysis. *Earth Surf. Process. Landforms* 38 (6), 570–576. doi:10.1002/esp.3302

Petrosino, P., Ermolli, E. R., Donato, P., Jicha, B., Robustelli, G., and Sardella, R. (2014). Using Tephrochronology and palynology to date the MIS 13 lacustrine sediments of the Mercure basin (Southern Apennines - Italy). *Italian J. Geosciences* 133 (2), 169–186. doi:10.3301/Ijg.2013.22

Piccarreta, M., Pasini, A., Capolongo, D., and Lazzari, M. (2013). Changes in daily precipitation extremes in the mediterranean from 1951 to 2010: The Basilicata region, southern Italy. *Int. J. Climatol.* 33 (15), 3229–3248. doi:10.1002/joc.3670

Poeppl, R. E., Coulthard, T., Keesstra, S. D., and Keiler, M. (2019). Modeling the impact of dam removal on channel evolution and sediment delivery in a multiple dam setting. *Int. J. Sediment Res.* 34 (6), 537–549. doi:10.1016/j.ijsrc.2019.06.001

Pritchard, D., Roberts, G. G., White, N. J., and Richardson, C. N. (2009). Uplift histories from river profiles. *Geophys. Res. Lett.* 36 (24), L24301. doi:10.1029/2009GL040928

Robustelli, G., Ermolli, E. R., Petrosino, P., Jicha, B., Sardella, R., and Donato, P. (2014). Tectonic and climatic control on geomorphological and sedimentary evolution of the Mercure basin, southern Apennines, Italy. *Geomorphology* 214, 423–435. doi:10.1016/j.geomorph.2014.02.026

Schiattarella, M., Di Leo, P., Beneduce, P., and Giano, S. I. (2003). Quaternary uplift vs tectonic loading: A case study from the lucanian apennine, southern Italy. *Quat. Int.* 101-102 (1), 239–251. doi:10.1016/s1040-6182(02)00126-x

Schiattarella, M., Giano, S. I., and Gioia, D. (2017). Long-term geomorphological evolution of the axial zone of the campania-lucania apennine, southern Italy: A review. *Geol. Carpathica* 68 (1), 57–67. doi:10.1515/geoca-2017-0005

Schiattarella, M., Giano, S. I., Gioia, D., Martino, C., and Nico, G. (2013). Age and statistical properties of the summit palaeosurface of southern Italy. *Geogr. Fis. E Din. Quat.* 36 (2), 289–302. doi:10.4461/Gfdq.2013.36.23

Schiattarella, M., Leo, P. D., Beneduce, P., Giano, S. I., and Martino, C. (2006). "Tectonically driven exhumation of a young orogen: An example from the southern Apennines, Italy," in *Tectonics, climate, and landscape evolution*. Editors S. D. Willett,

N. Hovius, M. T. Brandon, and D. Fisher (United States: Special Paper of the Geological Society of America), 398, 371–385.

Schiattarella, M., Torrente, M. M., and Russo, F. (1994). Analisi strutturale ed osservazioni morfostratigrafiche nel Bacino del Mercure (confine calabro-lucano). *Il Quat.* 7, 613–626.

Schmidt, J. L., Zeitler, P. K., Pazzaglia, F. J., Tremblay, M. M., Shuster, D. L., and Fox, M. (2015). Knickpoint evolution on the Yarlung river: Evidence for late Cenozoic uplift of the southeastern Tibetan plateau margin. *Earth Planet. Sci. Lett.* 430, 448–457. doi:10.1016/j.epsl.2015.08.041

Schoenbohm, L. M., Whipple, K. X., Burchfiel, B. C., and Chen, L. (2004). Geomorphic constraints on surface uplift, exhumation, and plateau growth in the Red River region, Yunnan Province, China. *Geol. Soc. Am. Bull.* 116 (7), 895. doi:10.1130/b25364.1

Skotnicki, S. J., Seong, Y. B., Dorn, R. I., Larson, P. H., DePonty, J., and Jeong, A. (2021). Drainage integration of the Salt and Verde rivers in a Basin and Range extensional landscape, central Arizona, USA. *Geomorphology* 374, 107512. doi:10.1016/j.geomorph.2020.107512

Soria-Jáuregui, A., Jiménez-Cantizano, F., and Antón, L. (2019). Geomorphic and tectonic implications of the endorheic to exorheic transition of the Ebro River system in northeast Iberia. *Quat. Res. (United States)* 91 (2), 472–492. doi:10.1017/qua.2018.87

Struth, L., Garcia-Castellanos, D., Viaplana-Muzas, M., and Vergés, J. (2019). Drainage network dynamics and knickpoint evolution in the Ebro and Duero basins: From endorheism to exorheism. *Geomorphology* 327, 554–571. doi:10.1016/j.geomorph.2018.11.033

Vacherat, A., Bonnet, S., and Mouthereau, F. (2018). Drainage reorganization and divide migration induced by the excavation of the Ebro basin (NE Spain). *Earth Surf. Dyn.* 6 (2), 369–387. doi:10.5194/esurf-6-369-2018

Wang, Y., Schoenbohm, L. M., Zhang, B., Granger, D. E., Zhou, R., Zhang, J., et al. (2017). Late Cenozoic landscape evolution along the Ailao Shan Shear Zone, SE Tibetan Plateau: Evidence from fluvial longitudinal profiles and cosmogenic erosion rates. *Earth Planet. Sci. Lett.* 472, 323–333. doi:10.1016/j.epsl.2017.05.030

Whipple, K. X. (2004). Bedrock rivers and the geomorphology of active orogens. *Annu. Rev. Earth Planet. Sci.* 32 (1), 151–185. doi:10.1146/annurev.earth.32.101802.120356

Whipple, K. X., and Tucker, G. E. (1999). Dynamics of the stream-power river incision model: Implications for height limits of mountain ranges, landscape response timescales, and research needs. *J. Geophys. Res. Solid Earth* 104 (B8), 17661–17674. doi:10.1029/1999JB900120

Willett, S. D., McCoy, S. W., Perron, J. T., Goren, L., and Chen, C.-Y. (2014). Dynamic reorganization of river basins. *Science* 343 (6175), 1248765. doi:10.1126/science.1248765

Wobus, C., Whipple, K. X., Kirby, E., Snyder, N., Johnson, J., Spyropolou, K., et al. (2006). "Tectonics from topography: Procedures, promise, and pitfalls," in *Special paper of the* (Colorado, United States: Geological Society of America).

Zembo, I. (2010). Stratigraphic architecture and quaternary evolution of the Val d'Agri intermontane basin (Southern Apennines, Italy). *Sediment. Geol.* 223 (3-4), 206–234. doi:10.1016/j.sedgeo.2009.11.011